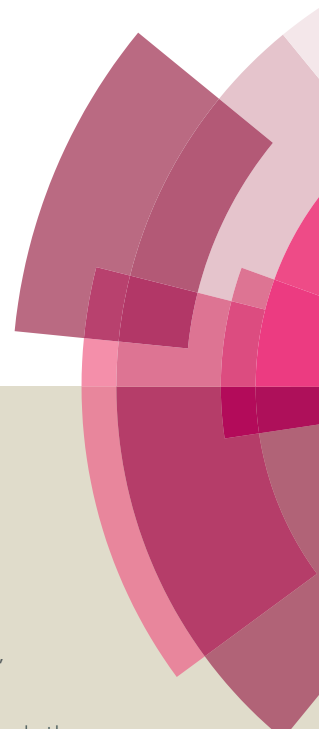


Journal of Materials Chemistry B

Accepted Manuscript



This article can be cited before page numbers have been issued, to do this please use: X. Zhang, J. Liu, W. Ma and M. Yang, *J. Mater. Chem. B*, 2016, DOI: 10.1039/C6TB01465H.



This is an *Accepted Manuscript*, which has been through the Royal Society of Chemistry peer review process and has been accepted for publication.

Accepted Manuscripts are published online shortly after acceptance, before technical editing, formatting and proof reading. Using this free service, authors can make their results available to the community, in citable form, before we publish the edited article. We will replace this *Accepted Manuscript* with the edited and formatted *Advance Article* as soon as it is available.

You can find more information about *Accepted Manuscripts* in the [Information for Authors](#).

Please note that technical editing may introduce minor changes to the text and/or graphics, which may alter content. The journal's standard [Terms & Conditions](#) and the [Ethical guidelines](#) still apply. In no event shall the Royal Society of Chemistry be held responsible for any errors or omissions in this *Accepted Manuscript* or any consequences arising from the use of any information it contains.



Journal Name

ARTICLE

Near-infrared fluorescence of π -conjugation extended benzothiazole and its application for biothiols imaging in living cells

Received 00th January 20xx,
Accepted 00th January 20xx

DOI: 10.1039/x0xx00000x

www.rsc.org/

Xuan Zhang,*^a Jing-Yun Liu,^{†a} Wei-Wei Ma^{†a} and Meng-Lu Yang^a

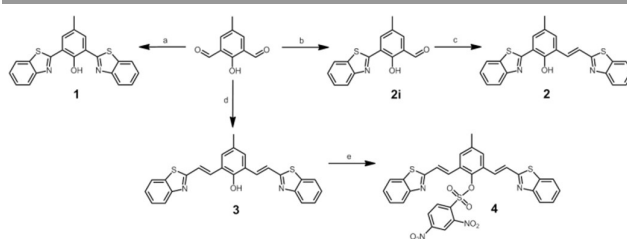
Two new π -conjugation extended benzothiazole derivatives bearing single (**2**) or double (**3**) vinyl groups between benzothiazolyl and 4-methylphenol moieties in 2,6-dibenzothiazolyl-4-methylphenol (**1**), have been synthesized and their photophysical properties were studied. In the nonpolar solvents, **2** showed a keto tautomer emission from the excited state intramolecular proton transfer (ESIPT) at 626 nm, remarkably red-shifted than the keto tautomer fluorescence of **1** (568 nm), whereas **3** only exhibited an enol emission at 420 nm. However, a near-infrared (NIR) emission at 616/688 nm for **2/3** from the deprotonated anion species was observed in polar solvent, which is farther red-shifted than that of deprotonated **1** (516 nm). With the aid of computational studies, the experimental observations were rationalized according to the efficient extension of π -conjugation of molecular backbone in **2** and **3**. Furthermore, a white emission with a broad band between 400 and 800 nm from **3** was also observed in a polar-nonpolar solvent mixture, where a near pure white coordinates (0.33, 0.35) from the CIE chromaticity diagram was successfully achieved. By masking the phenol group in **3**, a NIR fluorescent probe (**4**) for biothiols was constructed that allow to imaging application in living cells.

Introduction

The design and synthesis of organic fluorophores exhibiting near-infrared (NIR) fluorescence have attracted intense scientific interest due to their promising application in fluorescence imaging and sensing.¹ It has been well-known that the NIR fluorescence has many advantages such as deeper penetration ability, lower interference from tissue autofluorescence, and especially nondestructive.¹ Accordingly, many NIR fluorescent dyes have been developed based on various conjugated molecular skeletons. For example, cyanine, BODIPY, xanthene, porphyrin, and squaraine dyes have been extensively investigated in NIR fluorescence imaging and fluorescent probe design.² However, most of these classic NIR fluorescent dyes suffer from small Stokes shifts and sometimes low fluorescence quantum yields, preventing their practical application in bioimaging due to the low contrast.² Therefore, the development of the NIR fluorescent dyes with both high fluorescence quantum yield and large Stokes shift are highly desired. In this regard, much effort has been devoted to tuning the fluorescence emission properties of the above-mentioned NIR dyes by tailoring their π -conjugation.³ In addition, white

light emission generation from a single organic molecule is attracting considerable attention due to its potential on the development of white organic light-emitting diodes (WOLED), but it is still a challenging task.⁴

Recently, we and other researchers found that the excited state intramolecular proton transfer (ESIPT) fluorescence emission color of 2-(2-hydroxyphenyl) benzothiazole (HBT) could be efficiently modulated from green to yellow, by extending the π -conjugation in bis-HBT such as 2,6-dibenzothiazolyl-4-methylphenol (**1**, Scheme 1) and tris-HBT derivatives, where the second and third benzothiazolyl groups were attached on phenol moiety respectively.⁵ It is therefore intriguing to expect that the further extending of the π -conjugation backbone by introducing the vinyl group between benzothiazolyl and 4-methylphenol moiety in **1**, would shift the emission into the NIR region. In this work, two novel π -conjugation extended benzothiazole derivatives (**2** and **3**, Scheme 1) were synthesized and their photophysical



Scheme 1 Synthesis of **1–4**. Reagents and conditions: (a) 2-aminobenzeneethiol, DMSO, 180 °C, 2 h; (b) 2-aminobenzeneethiol, THF, r.t., 72 h; (c, d) 2-methylbenzothiazole, AcO₂, 80 °C, 12 h; 15% NaOH, 85 °C, 1 h; HCl, pH = 7; (e) Na₂CO₃, CH₂Cl₂, 2,4-dinitrobenzenesulfonyl chloride, r.t., 6 h.

^a College of Chemistry, Chemical Engineering & Biotechnology, Donghua University, Shanghai 201620, China. E-mail: xzhang@dhu.edu.cn

[†] These authors contributed equally to this work.

‡ Electronic Supplementary Information (ESI) available: ¹H NMR, ¹³C NMR, and MALDI-TOF-MS spectra of benzothiazole derivatives **2–4**, ESI-MS spectra of **4** in the absence and presence of Cys, and calculated MO for the excited K* of **1** and **2**. See DOI: 10.1039/x0xx00000x

ARTICLE

properties were investigated experimentally and theoretically, in comparison with those of **1**. It was found that **2** showed a longer keto tautomer emission at 626 nm, remarkably red-shifted than that of **1** (568 nm), whereas **3** exhibited a NIR emission at 688 nm from the deprotonated anion species, farther red-shifted than that of deprotonated **1** (516 nm). Furthermore, a white emission generation was achieved from **3** in a polar-nonpolar solvent mixture, and by masking the phenol group in **3**, a NIR fluorescent probe (**4**, Scheme 1) was constructed for biothiols imaging in living cells.

Results and discussion

Synthesis of π -conjugation extended benzothiazole derivatives

The synthesis of **1–4** was accomplished using strategies as shown in Scheme 1. Starting material 2,6-diformyl-4-methylphenol was facilely synthesized from commercial available 4-methylphenol via Duff reaction according to the previously established procedure.^{5a} The derivative **1** and intermediate aldehyde **2i** were obtained by direct condensation reaction between 2,6-diformyl-4-methylphenol with 2-aminobenzenethiol as previously described,^{5a} whereas **2** and **3** were prepared by condensation reaction between the corresponding aldehyde with commercially available 2-methylbenzothiazole. Then **3** was reacted with 2,4-dinitrobenzenesulfonyl chloride in the presence of Na_2CO_3 to provide the probe **4**. The synthesis details were presented in the Experimental section.

Photophysical properties of benzothiazole derivatives

The absorption and fluorescence spectra of benzothiazole derivatives **2** and **3** were measured in various solvents such as hexane, CHCl_3 and DMF and the results are shown in Fig. 1 and Table 1, where the corresponding data of compound **1** were also included for comparison. Obviously, all compounds exhibit solvent-dependent photophysical properties. In nonpolar solvents hexane and CHCl_3 , compounds **1–3** show absorption bands at 300–450 nm (Figs. 1b and d), and the low energy absorption bands are ascribed to the $S_0 \rightarrow S_1$ ($\pi\pi^*$) transitions from enol conformers ($E \rightarrow E^*$, Schemes 2 and 3). E conformer is a closed form in **2** due to an intramolecular hydrogen-bonding involved as observed in **1**, but **3** adopts an open form (Schemes 2 and 3). Notably, the low energy absorption band of **2** is slightly red-shifted than that of **1**, implying a longer π -conjugation length in the former. However, in polar solvent DMF, new lower energy absorption bands appeared around 400–650 nm for **1–3** (Fig. 1f), which can be attributed to the deprotonated anion conformers ($A \rightarrow A^*$, Schemes 2 and 3). It is known that F^- is a strong proton acceptor, which could easily induce a deprotonation of phenol in organic solvent.⁶ Similar absorption spectra were observed in the presence of F^- in CHCl_3 (Fig. 1h), further confirming the occurrence of deprotonation in **1–3** in polar solvent DMF. Interestingly, the wavelength of anion absorption follows the order of **3** (580 nm) > **2** (528 nm) > **1** (491 nm), suggesting that the π -conjugation is efficiently extended by introducing vinyl group.

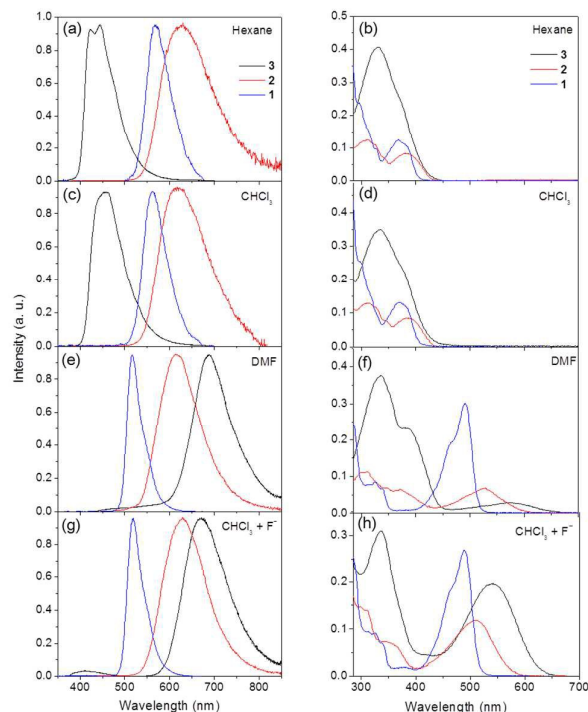
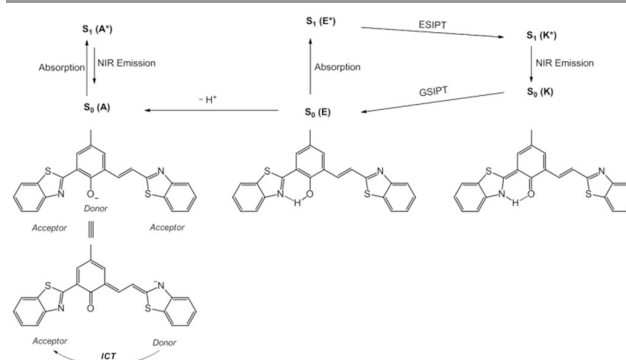
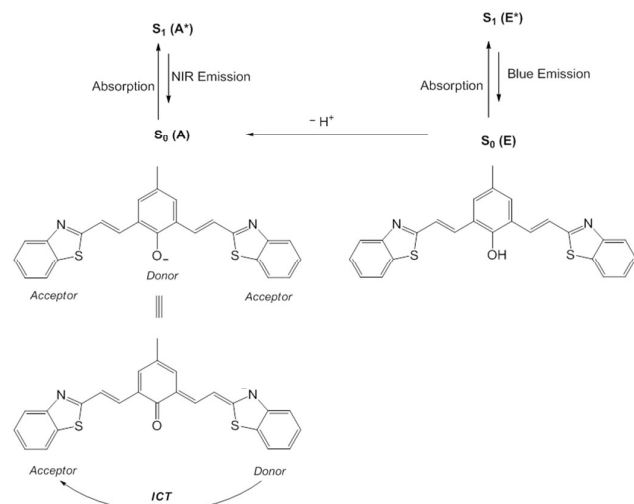


Fig. 1 Absorption (b, d, f, h) and fluorescence (a, c, e, g) spectra of **1–3** in various solvents (a–f) and in the presence of F^- in CHCl_3 (g, h). Excitation wavelength is 345 nm.

On the other hand, **2** shows a broad emission band around 620 nm in nonpolar solvents hexane and CHCl_3 with a large Stokes-shift of ca. 10000 cm^{-1} (Figs. 1a and c), similar to that observed in **1**, which is a typical characteristic of ESIPT emission from keto tautomer ($K^* \rightarrow K$, Scheme 2). As shown in Scheme 2, the K^* state of **2** was derived from E^* state via an ESIPT process, relaxed to ground state (K) through ESIPT emission and followed by back ground state intramolecular proton transfer (GSIPT) to the more stable E state.⁷ The longer keto emission wavelength of **2** than that of **1** is consistent with the longer π -conjugation length in the former. In contrast, **3** shows a blue emission around 450 nm in nonpolar solvents hexane and CHCl_3 due to the absence of ESIPT process (Figs. 1a and c, Table 1), ascribed to enol conformer ($E^* \rightarrow E$, Scheme 3). In polar DMF, **2** shows a blue-shifted emission at 616 nm as



Scheme 2 Schematic representation of the photophysical processes for **2**.



Scheme 3 Schematic representation of the photophysical processes for **3**.

similarly observed in **1**, whereas **3** exhibits a strongly red-shifted NIR fluorescence emission at 688 nm, accompanied by a 2-folds enhancement of fluorescence quantum yield (Fig. 1e, Table 1). In consistent with absorption spectra, the emissions in polar DMF can be ascribed to the deprotonated anion conformers ($A^* \rightarrow A$, Schemes 2 and 3), which is further confirmed by the similar emission spectra in the presence of strong proton acceptor F^- in $CHCl_3$ (Fig. 1g). It has been known that phenol moiety acts as a latent donor when it is conjugated with two acceptors, but deprotonation of phenol will transform it into an active phenolate donor and thus switch on intramolecular charge transfer (ICT) emission.^{1c} Therefore, as illustrated in Schemes 2 and 3, the NIR emissions of **2** and **3** in DMF can be similarly explained by following ICT mechanism (Schemes 2 and 3). Notably, the wavelength of anion emission follows the order of **3** (688 nm) > **2** (616 nm) > **1** (516 nm), which is in agreement with the order of π -conjugation length.

Theoretical calculations

In order to further understand the photophysical properties of compounds **1–3**, we performed a computation study on their absorption and the fluorescence spectra by DFT/TDDFT calculations at the B3LYP/6-31+G(d) level. The results are summarized in Table 2. The calculated absorption (for E and A) and emission (for K^* and A^*) maximum wavelengths of **1–3**

(Table 2) reproduced well the observed experimental trends (Table 1 and Fig. 1), allowed the theoretical analysis of the factors responsible for the variation of photophysical properties. It can be seen that both the predicted wavelengths and intensities increase with elongation of the π -conjugation

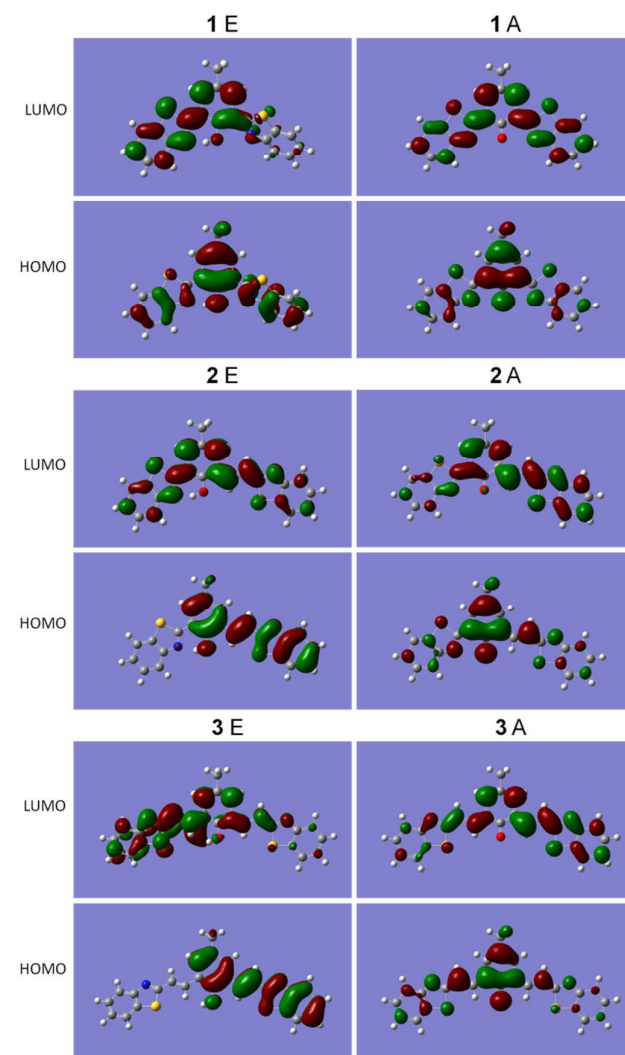


Fig. 2 HOMO and LUMO orbitals of enol (E) and anion (A) conformers of **1–3** in the ground state.

Table 1 Photophysical properties of compounds **1–3** in various solvents

Compounds	solvents	λ_{Abs}^a (nm)	ϵ^b ($M^{-1} cm^{-1}$)	λ_{Flu}^c (nm)	Φ_F^d
1 ^e	Hexane	369	12420	568	0.029
	$CHCl_3$	370	12990	560	0.086
	DMF	325/491	8670/30250	516	0.381
2	Hexane	312/383	12510/8450	626	0.058
	$CHCl_3$	315/387	13680/8700	620	0.104
	DMF	306/528	11470/7180	616	0.242
3	Hexane	331/375(sh.) ^f	40950/-	435	0.218
	$CHCl_3$	335/380(sh.) ^f	34970/-	455	0.210
	DMF	336/386(sh.) ^f /580	37890/23310/2800	688	0.454
	PBS ^g	335/386(sh.) ^f /500	31080/-/10350	670	0.111

^aThe maximum absorption wavelength. ^bThe molar absorption coefficient. ^cThe maximum fluorescence emission wavelength ($\lambda_{ex} = 315$ nm for **2**, 331 nm for **3**). ^dThe fluorescence quantum yield measured by using quinine sulfate as a standard. ^eTaken from ref. 5a. ^fShoulder peak. ^g10 mM PBS containing 50% EtOH.

Table 2 Theoretical electronic properties of compounds **1–3** calculated at TDDFT/B3LYP/6-31+g (d, p) level in the gas phase, based on the optimized ground (for absorption) and excited states (for fluorescence) geometries (gas phase). Calculated enol/anion (E/A) absorption and keto/anion (K*/A*) emission transitions (nm, eV) and oscillator strength (*f*).

Compounds	Abs (E / A)			Flu (K* / A*)		
	nm	eV	<i>f</i>	nm	eV	<i>f</i>
1	367/516	3.38/2.40	0.40/0.67	624/560	1.99/2.22	0.28/0.53
2	389/586	3.18/2.12	0.71/0.83	633/648	1.96/1.91	0.44/0.63
3	376/635	3.30/1.95	1.07/1.00	NA ^a /679	NA ^a /1.82	NA ^a /0.88

^a Not applicable.

by addition of vinyl double bonds to the conjugated backbone of benzothiazole derivative **1**. Shapes of the ground state frontier orbitals of E and A of **1–3** (Fig. 2) are respectively similar, where both the highest occupied molecular orbital (HOMO) and the lowest unoccupied molecular orbital (LUMO) are almost distributed on whole molecular backbone, suggesting a predominant π - π^* transition character. More significant delocalization occurred in the A conformer and the length of conjugation backbone is followed the order of **3** A > **2** A > **1** A. That explains well the corresponding π -conjugation length-dependent absorption and emission spectra of A species in polar DMF solvent (Figs. 1e and f). On the other hand, the excited state frontier orbitals of K* of **2** showed the longer π -conjugation length than that of **1** (Fig. S1†), which is responsible for the longer ESIPT emission of **2** observed in nonpolar solvents (Figs. 1a and c, Table 1). Therefore, elongation of the conjugated backbone in benzothiazole derivative is a promising strategy to shift the fluorescence to the NIR region, as also shown in experimental results given in Table 1.

White emission

From nonpolar to polar solvents, the fluorescence of **3** changed from blue to NIR that covers almost entire visible region, making it promising to be utilized for producing white emission in nonpolar-polar binary solvent. As a consequence, when DMF was gradually added into the CHCl₃ solution of **3**, the original blue emission around 400–600 nm decreased with increasing of NIR emission at 600–800 nm (Fig. 3a). At a ratio of 7:3 (CHCl₃:DMF), a white emission covered 400–800 nm was successfully created (Fig. 3a). Further increasing the DMF proportions leads to the predominant NIR emission. The CIE chromaticity diagram (Fig. 3b) clearly shows the blue-white-red fluorescence color change with the ratio of CHCl₃ to DMF, where near pure white coordinates (0.33, 0.33) were obtained at the ratio of 7:3 (0.33, 0.35). Obviously, white light emission generation from a single organic molecule is successfully achieved in our designed compound **3**.

Fluorescence sensing of biothiols and imaging in living cells

The anion conformation of **3** showed the NIR fluorescence with high quantum yield and large Stokes shift, making it promising for developing the NIR fluorescent probe by masking of the active phenol group. Such design strategy has been usually used in turn-on mode fluorescent probe by analyte-induced removal of the masking group.⁸ Therefore, we synthesized **4** by masking the active phenol group of **3** with a

notorious fluorescence quencher, 2,4-dinitrobenzenesulfonate moiety that is well-known reactive towards biological thiols such as cysteine (Cys), homocysteine (Hcy) and glutathione (GSH).⁹ As shown in Fig. 4a, the probe **4** exhibits a significant NIR fluorescence enhancement towards Cys, Hcy and GSH in a phosphate buffer (10 mM PBS containing 50% EtOH, pH = 7.4), but not towards other amino acids and common ions. Furthermore, Cys showed the larger enhancement and the reaction finished within 30 min (Fig. 4). To confirm the probe **4** has been transformed into **3** in the presence of Cys as shown

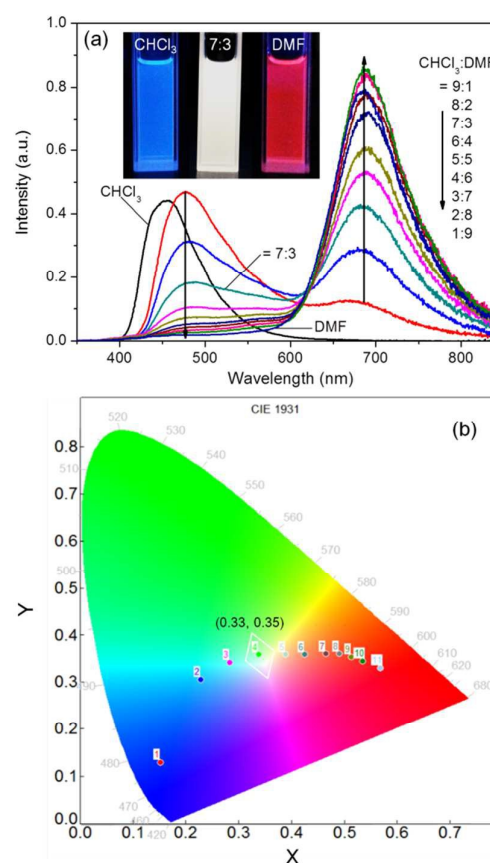


Fig. 3 Fluorescence spectral change ($\lambda_{\text{exc}} = 345$ nm) of **3** by changing the CHCl₃/DMF ratio from 10:0 to 0:10 (a). The corresponding CIE chromaticity diagram, where the coordinate of (0.33, 0.35) was obtained at the ratio of 7:3 that is near pure white coordinates (0.33, 0.33) (b). Insets in (a) are photographs of **3** in CHCl₃, 7:3 CHCl₃/DMF, and DMF under a UV lamp (365 nm) irradiation, respectively.

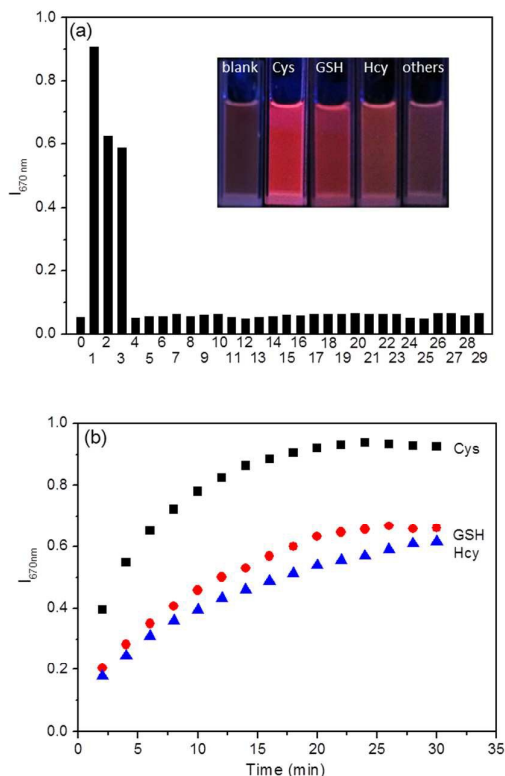
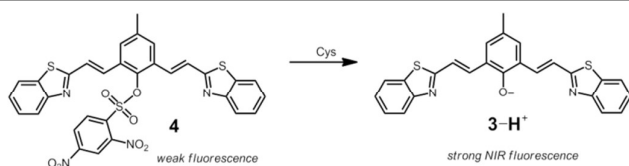


Fig. 4 Fluorescence intensity change ($\lambda_{\text{ex}} = 345 \text{ nm}$, $\lambda_{\text{em}} = 670 \text{ nm}$) of the probe **4** (10 μM) in the absence and presence of 2 equiv. of various amino acids and biologically relevant species in aqueous PBS buffer (pH = 7.4) (a), where the number of 0-29 represents probe **4** only and in the presence of Cys, GSH, Hcy, Ser, Val, His, Arg, Hyp, Ala, Glu, Gln, Met, Asp, Asn, Pro, Leu, Lys, Ile, Phe, Tyr, Thr, Trp, Gly, Tau, Glucose, Na^+ , K^+ , Mg^{2+} , Ca^{2+} , respectively. Response time course of fluorescence intensity of the probe **4** in the presence of Cys, GSH and Hcy, respectively (b). Insets in (a) are solutions of **4** alone and in the presence of Cys, GSH, Hcy and other species test in this work by exposing to a UV lamp at 365 nm.



Scheme 4 The proposed reaction mechanism of the probe **4** with Cys.

in Scheme 4, ESI-mass spectrum analysis of the product generated from the incubation of **4** with Cys in EtOH–H₂O (1 : 1, v/v) solution. A prominent peak at $m/z = 425.0$ corresponding to $[\mathbf{3} - \text{H}^+]^-$ is clearly observed in the ESI-MS spectrum, whereas only a prominent peak at $m/z = 679.5$ corresponding to $[\mathbf{4} + \text{Na}]^+$ appeared in the absence of Cys (Fig. S2 \ddagger). This provides strong evidence that Cys-induced deprotection reaction occurs, leading to a recovery of strong NIR fluorescence (Scheme 4). As shown in Fig. 5, the NIR fluorescence at 670 nm was gradually increased upon addition of Cys and leveled off when the concentration of Cys reached 50 μM , and a good linear relationship was obtained over the

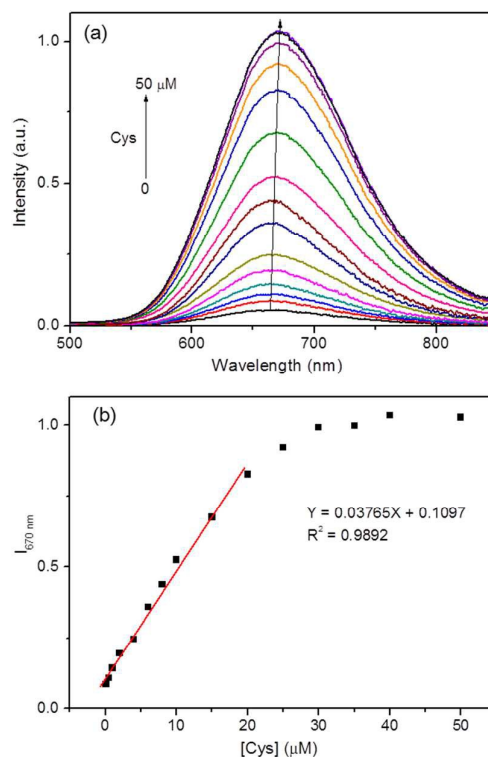


Fig. 5 Change of fluorescence spectra of **4** (10 μM) with addition of various amounts of Cys (0–50 μM) (a). The corresponding linear relationship between the fluorescence intensity at 670 nm and concentration of Cys (0.2–20 μM) (b).

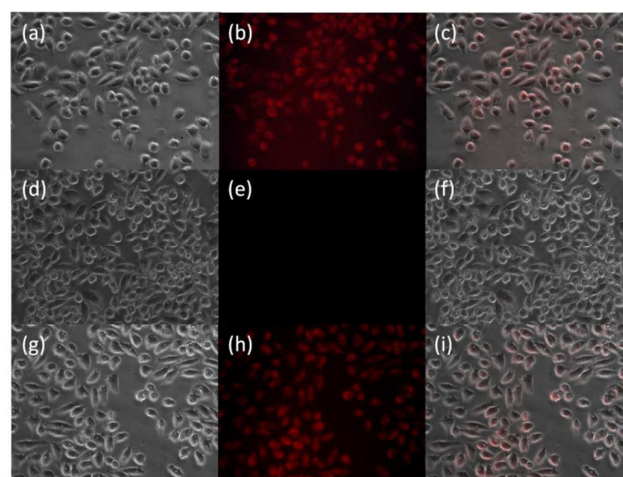


Fig. 6 Confocal fluorescence images of living fibroblast L929 cells incubated with the probe **4** (10 μM) for 30 min at 37 $^{\circ}\text{C}$: cells without treatment (a, b, c), cells with pre-treatment of NEM (1 mM) (d, e, f), and cells with pre-treatment of NEM (1 mM) and addition of 30 μM Cys (g, h, i). (a, d, g) are the bright-field images; (b, e, h) are the fluorescence images; (c, f, i) are the overlap of the fluorescence and bright-field images.

range of 0.2–20 μM . The detection limit was estimated to be 0.1 μM according to $S/N = 3$, which shows a better or comparable sensitivity to those reported previously.^{2g,2e,3c,8c,8e,10} The intracellular Cys concentration has

ARTICLE

Journal Name

been reported to be on the level of 30–200 μM ,^{10d} indicating the probe **4** is sensitive enough to image Cys in living cells.

Biological thiols (Cys, Hcy and GSH) play crucial roles in maintaining redox balance of biological systems, for example, abnormal levels of Cys could cause edema, lethargy, liver damage, etc., and therefore their imaging in living cells have received many recent attention.^{10,11} To verify the potential application in living cells imaging, the fibroblast L929 cells were incubated with probe **4** at 37 °C for 30 min and observed by confocal fluorescence microscope (Fig. 6). As shown in Fig. 6b, a bright red fluorescence was observed inside the cells, indicating the intracellular thiols induced a deprotection and a recovery of strong NIR fluorescence. In contrast, when the cells were pre-treated with addition of N-ethylmaleimides (NEM, 1 mM), a known thiol-blocking agent, and then incubated with probe **4** for 30 min, almost no fluorescence was detected (Fig. 6e), but further incubation with 30 μM Cys leads to an appearance of bright red fluorescence (Fig. 6h). This indicates that the probe **4** can be applied to image biothiols in living cells.

Conclusions

In summary, by introducing vinyl group, two new π -conjugation extended benzothiazole derivatives (**2** and **3**) have been synthesized and their photophysical properties were investigated by comparison with that of the parent molecule **1**. It was found that **2** showed an ES IPT emission at 626 nm, whereas **3** exhibited an enol emission at 420 nm in the nonpolar solvents. However, a NIR emission at 616/688 nm for **2/3** from the deprotonated anion species was observed in polar solvent, which is farther red-shifted than that of deprotonated **1** (516 nm). With the aid of computational studies, the experimental observations were rationalized according to the efficient extension of π -conjugation of molecular backbone in **2** and **3**. A white emission with a broad band between 400 and 800 nm from **3** was observed in a polar-nonpolar binary solvents, where a near pure white coordinates (0.33, 0.35) from the CIE chromaticity diagram was successfully achieved. By masking the phenol group in **3**, a NIR fluorescent probe (**4**) for biothiols was constructed that allow to imaging application in living cells. Thus these findings will contribute to designing new NIR fluorescent dyes with large Stokes shift and high fluorescence quantum yield, and developing NIR fluorescent probes for biological imaging application.

Experimental

Materials and Measurements

All the chemicals are analytical grade and purchased from Sinopharm Chemical Reagents Co. (Shanghai). Fluorescence spectra were measured on Edinburgh FS5 spectrofluorometer with Ex/Em slit widths of 2.5 nm. Absorption spectra were obtained on PerkinElmer Lambda 35 UV/VIS spectrophotometer. The fluorescence quantum yield in

solution was determined by using quinine sulfate ($\Phi_f = 0.546$ in 0.1 M H_2SO_4) as a standard.¹² ^1H NMR and ^{13}C NMR spectra were recorded on a Bruker AVANCE III 400 MHz spectrometer with TMS as standard. Mass spectra were obtained on AB Sciex MALDI-TOF/TOFTM MS or a Varian 310 spectrometer, respectively. Confocal fluorescence imaging experiments in living fibroblast L929 cells were carried out with a Carl Zeiss LSM 700 microscope.

Synthesis

Compound **1** was obtained according to the previously reported procedure.⁵

Synthesis of 2. 2,6-diformyl-4-methylphenol (2 mmol) and 2-aminobenzenethiol (0.5 mmol) were dissolved in EtOH (15 mL) and THF (15 mL) and stirred under an N_2 atmosphere at room temperature for 72 h. The intermediate aldehyde **2i** was obtained by column chromatography (silica gel, hexane/ethyl acetate = 20:1 v/v) and used directly for the next step. Then **2i** (0.05 mmol) and 2-methylbenzothiazole (0.5 mmol) were dissolved in acetic anhydride (2 mL) and refluxed for 10 hours. After cooling to the room temperature, sodium hydroxide solution (50 mL, 15%) was added and the mixture was heated to 85 °C for 1 h. The solution pH was adjusted to about 7 by adding HCl solution (35%). The crude product was collected by filtration and purified by column chromatography (silica gel, hexane/ethyl acetate = 20:1 v/v) to give **2** as yellow solid. Yield: 5%. ^1H NMR (400 MHz, CDCl_3), δ (ppm): 13.30 (s, 1H), 8.10 (t, $J = 12$ Hz, 2H), 8.03 (d, $J = 8$ Hz, 1H), 7.95 (d, $J = 8$ Hz, 1H), 7.90 (d, $J = 8$ Hz, 1H), 7.77 (d, $J = 16$ Hz, 1H), 7.59–7.42 (m, 6H), 2.43 (s, 3H), ^{13}C NMR (100 MHz, CDCl_3), δ (ppm): 169.14, 168.15, 154.59, 151.64, 134.14, 133.14, 132.61, 131.69, 129.74, 128.64, 126.82, 126.37, 125.72, 125.37, 124.15, 122.77, 122.70, 122.19, 121.54, 116.99, 20.60. MALDI-TOF-MS: m/z calcd 400.52; found 400.81.

Synthesis of 3. Under an N_2 atmosphere, 2,6-diformyl-4-methylphenol (2 mmol) and 2-methylbenzothiazole (5 mmol) were refluxed in acetic anhydride (2 mL) for 12 hours. After cooling to the room temperature, sodium hydroxide solution (50 mL, 15%) was added and the mixture was heated to 85 °C for 1 h. The solution was adjusted to about 7 by adding HCl solution (35%). The crude product was collected by filtration and purified by column chromatography (silica gel, hexane/ethyl acetate = 10:1 v/v) to give **3** as yellow solid. Yield: 5%. ^1H NMR (400 MHz, DMSO-d_6), δ (ppm): 9.88 (s, 1H), 8.11 (d, $J = 8$ Hz, 2H), 8.04 (s, 1H), 7.99 (t, $J = 4$ Hz, 3H), 7.69 (s, 2H), 7.59 (d, $J = 16$ Hz, 2H), 7.53 (t, $J = 8$ Hz, 2H), 7.45 (t, $J = 8$ Hz, 2H), 2.34 (s, 3H); ^{13}C NMR (100 MHz, DMSO-d_6), δ (ppm): 167.48, 153.99, 134.48, 133.12, 129.27, 125.19, 122.94, 122.63, 122.10, 20.67. MALDI-TOF-MS: m/z calcd 426.55; found 426.94.

Synthesis of 4. Under an N_2 atmosphere, **3** (0.5 mmol) was dissolved in 10 mL dichloromethane, and Na_2CO_3 (2 mmol) and 2,4-dinitrobenzenesulfonyl chloride (1.5 mmol) were added and the mixture solution was then stirred for at room temperature for 6 h. The crude product was obtained by extracting with chloroform, drying with MgSO_4 and evaporating. The product was further purified by column chromatography (silica gel, hexane/ethyl alcohol=, 10:1 v/v).

Yield: 75%. ^1H NMR (400 MHz, CDCl_3), δ (ppm): 8.32 (s, 1H), 8.26 (d, $J = 8\text{ Hz}$, 1H), 8.10 (s, 1H), 8.07 (t, $J = 6\text{ Hz}$, 2H), 7.91 (d, $J = 8\text{ Hz}$, 2H), 7.72 (d, $J = 16\text{ Hz}$, 2H), 7.60 (t, $J = 6\text{ Hz}$, 4H), 7.51 (t, $J = 8\text{ Hz}$, 2H), 7.39 (d, $J = 16\text{ Hz}$, 2H), 2.52 (s, 3H); ^{13}C NMR (100 MHz, CDCl_3), δ (ppm): 150.35, 143.87, 138.86, 134.48, 133.60, 131.09, 130.54, 128.94, 127.06, 126.46, 126.30, 125.01, 124.99, 122.97, 121.77, 120.74, 21.26. MALDI-TOF-MS: m/z calcd 656.71; found 656.62.

Calculations

All theoretical calculations were carried out using Gaussian 09 package.¹³ The ground state (S_0) and the first singlet excited state (S_1) geometries of the compounds were firstly optimized in the gas phase using density functional theory (DFT) and time-dependent density functional theory (TDDFT) at the B3LYP/6-31+G(d) level, respectively. Then the absorption and fluorescence emission properties were calculated with TDDFT based on the optimized S_0 and S_1 state geometries, respectively.

Cell imaging

Fibroblast L929 cells were cultured in Dulbecco's Modified Eagle's Medium (DMEM) supplemented with 10% fetal bovine serum (FBS) in 5% CO_2 and 95% humidity atmosphere at 37 °C. L929 cells were incubated with the probe **4** (10 μM) for 30 min at 37 °C and washed three times with PBS to remove the remaining probe, and then observed under a Carl Zeiss LSM 700 fluorescence microscope. For control experiments, L929 cells were pre-treated with N-ethylmaleimide (NEM, 1 mM) for 30 min at 37 °C, washed three times with PBS, and further incubated with the probe **4** (10 μM) or with Cys (30 μM) prior to addition of probe **4** for 30 min. Cells were then washed three times with PBS and used for fluorescence imaging.

Acknowledgements

This work was financially supported by Shanghai Municipal Natural Science Foundation (16ZR1401700) and Fundamental Research Funds for the Central Universities (No.2232014D3-11). We would like to appreciate Dr. Xiao-Yue Zhu and Prof. Xiang-Yang Shi for their kind assistances on cell imaging.

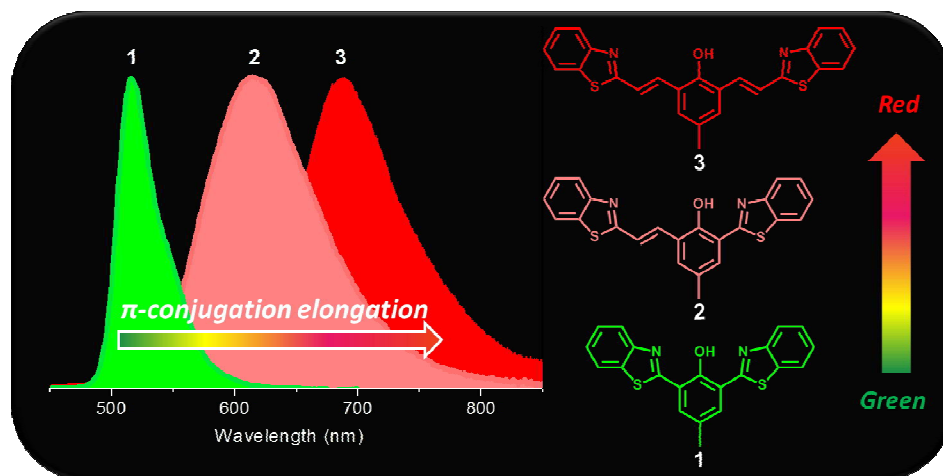
Notes and references

- (a) D. D. Nolting, J. C. Gore and W. Pham, *Curr. Org. Synth.*, 2011, **8**, 521–534; (b) Y. Yang, Q. Zhao, W. Feng and F. Li, *Chem. Rev.*, 2013, **113**, 192–270; (c) N. Karton-Lifshin, L. Albertazzi, M. Bendikov, P. S. Baran and D. Shabat, *J. Am. Chem. Soc.*, 2012, **134**, 20412–20420; (d) L. Yuan, W. Lin, K. Zheng, L. He and W. Huang, *Chem. Soc. Rev.*, 2013, **42**, 622–661; (e) Z. Guo, S. Park, J. Yoon and I. Shin, *Chem. Soc. Rev.*, 2014, **43**, 16–29; (f) S. Luo, E. Zhang, Y. Su, T. Cheng and C. Shi, *Biomaterials*, 2011, **32**, 7127–7138.
- (a) X. Wang, L. Cui, N. Zhou, W. Zhu, R. Wang, X. Qian and Y. Xu, *Chem. Sci.*, 2013, **4**, 2936–2940; (b) Y.-Q. Sun, J. Liu, X. Lv, Y. Liu, Y. Zhao and W. Guo, *Angew. Chem., Int. Ed.*, 2012, **51**, 7634–7636; (c) J. Chen, W. Liu, B. Zhou, G. Niu, H. Zhang, J. Wu, Y. Wang, W. Ju and P. Wang, *J. Org. Chem.*, 2013, **78**, 6121–6130; (d) F. Kong, R. Liu, R. Chu, X. Wang, K. Xu and B. Tang, *Chem. Commun.*, 2013, **49**, 9176–9178; (e) H. Lv, X.-F. Yang, Y. Zhong, Y. Guo, Z. Li and H. Li, *Anal. Chem.*, 2014, **86**, 1800–1807; (f) J. Yin, Y. Kwon, D. Kim, D. Lee, G. Kim, Y. Hu, J.-H. Ryu and J. Yoon, *J. Am. Chem. Soc.*, 2014, **136**, 5351–5358; (g) K. Yin, F. Yu, W. Zhang and L. Chen, *Biosens. Bioelectro.*, 2015, **74**, 156–164; (h) Y. Ding, Y. Tang, W. Zhu and Y. Xie, *Chem. Soc. Rev.*, 2015, **44**, 1101–1112; (i) Y.-J. Gong, X.-B. Zhang, G.-J. Mao, L. Su, H.-M. Meng, W. Tan, S. Feng and G. Zhang, *Chem. Sci.*, 2016, **7**, 2275–2285.
- (a) L. Yuan, W. Lin, S. Zhao, W. Gao, B. Chen, L. He and S. Zhu, *J. Am. Chem. Soc.*, 2012, **134**, 13510–13523; (b) X. Xiong, F. Song, G. Chen, W. Sun, J. Wang, P. Gao, Y. Zhang, B. Qiao, W. Li, S. Sun, J. Fan and X. Peng, *Chem.–Eur. J.*, 2013, **19**, 6538–6545; (c) J. Zhang, J. Wang, J. Liu, L. Ning, X. Zhu, B. Yu, X. Liu, X. Yao and H. Zhang, *Anal. Chem.*, 2015, **87**, 4856–4863; (d) Y. Hiruta, H. Koiso, H. Ozawa, H. Sato, K. Hamada, S. Yabushita, D. Citterio and K. Suzuki, *Org. Lett.*, 2015, **17**, 3022–3025; (e) Y. Li, Y. Wang, S. Yang, Y. Zhao, L. Yuan, J. Zheng and R. Yang, *Anal. Chem.*, 2015, **87**, 2495–2503; (f) H. Chen, W. Lin, H. Cui, W. Jiang, *Chem.–Eur. J.*, 2015, **21**, 733–745; (g) Y. Wei, D. Cheng, T. Ren, Y. Li, Z. Zeng and L. Yuan, *Anal. Chem.*, 2016, **88**, 1842–1849.
- (a) S. Mukherjee and P. Thilagar, *Dyes Pigm.*, 2014, **110**, 2–27; (b) Y. Liu, M. Nishiura, Y. Wang and Z. Hou, *J. Am. Chem. Soc.*, 2006, **128**, 5592–5593; (c) X.-H. Jin, C. Chen, C.-X. Ren, L.-X. Cai and J. Zhang, *Chem. Commun.*, 2014, **50**, 15878–15881; (d) J. Cheng, D. Liu, J. Bao, K. Xu, Y. Yang and K. Han, *Chem.–Asian J.*, 2014, **9**, 3215–3220; (e) W. Sun, S. Li, R. Hu, Y. Qian, S. Wang and G. Yang, *J. Phys. Chem. A*, 2009, **113**, 5888–5895; (f) K.-I. Sakai, S. Tsuchiya, T. Kikuchi and T. Akutagawa, *J. Mater. Chem. C*, 2016, **4**, 2011–2016.
- (a) X. Zhang and J.-Y. Liu, *Dyes Pigm.*, 2016, **125**, 80–88; (b) K.-I. Sakai, T. Ishikawa and T. Akutagawa, *J. Mater. Chem. C*, 2013, **1**, 7866–7871.
- (a) X. Zhang, L. Guo, F.-Y. Wu and Y.-B. Jiang, *Org. Lett.*, 2003, **15**, 2667–2670; (b) X. Peng, Y. Wu, J. Fan, M. Tian and K. Han, *J. Org. Chem.*, 2005, **70**, 10524–10531; (c) X. Zhang, Y. Shiraishi and T. Hirai, *Tetrahedron Lett.*, 2007, **48**, 8803–8806.
- (a) S. J. Formosinho, and L. G. Arnaut, *J. Photochem. Photobiol. A*, 1993, **75**, 21–48; (b) P. Majumdar and J. Zhao, *J. Phys. Chem. B*, 2015, **119**, 2384–2394; (c) Z. Yuan, Q. Tang, K. Sreenath, J. T. Simmons, A. H. Younes, D. Jiang and L. Zhu, *Photochem. Photobiol.*, 2015, **91**, 586–598.
- (a) Y. Tang, D. Lee, J. Wang, G. Li, J. Yu, W. Lin and J. Yoon, *Chem. Soc. Rev.*, 2015, **44**, 5003–5015; (b) X.-F. Yang, Q. Huang, Y. Zhong, Z. Li, H. Li, M. Lowry, J. O. Escobedo and R. M. Strongin, *Chem. Sci.*, 2014, **5**, 2177–2183; (c) Y. Liu, D. Yu, S. Ding, Q. Xiao, J. Guo and G. Feng, *ACS Appl. Mater. Interfaces*, 2014, **6**, 17543–17550; (d) S.-Y. Lim, K.-H. Hong, D. Il Kim, H. Kwon and H.-J. Kim, *J. Am. Chem. Soc.*, 2014, **136**, 7018–7025; (e) Y. Kim, M. Choi, S. Seo, S. T. Manjare, S. Jone and D. G. Churchill, *RSC Adv.*, 2014, **4**, 64183–64186; (f) H.-M. Lv, D.-H. Yuan, W. Liu, Y. Chen, C.-T. Au and S.-F. Yin, *Sens. Actuators B*, 2016, **233**, 173–179.
- (a) H. Maeda, H. Matsuno, M. Ushida, K. Katayama and K. Saeki, *Angew. Chem., Int. Ed.*, 2005, **44**, 2922–1903; (b) X. Chen, Y. Zhou, X. Peng and J. Yoon, *Chem. Soc. Rev.*, 2010, **39**, 2120–2135; (c) L.-Y. Niu, Y.-Z. Chen, H.-R. Zheng, L.-Z. Wu, C.-H. Tung and Q.-Z. Yang, *Chem. Soc. Rev.*, 2015, **44**, 6143–6160; (d) H. S. Jung, X. Chen, J. S. Kim and J. Yoon, *Chem. Soc. Rev.*, 2013, **42**, 6019–6031; (e) H. Chen, Y. Tang, M. Ren and W. Lin, *Chem. Sci.*, 2016, **7**, 1896–1903.
- (a) B. Liu, J. Wang, G. Zhang, R. Bai and Y. Pang, *ACS Appl. Mater. Interfaces*, 2014, **6**, 4402–4407; (b) D. Lee, G. Kim, J. Yin and J. Yoon, *Chem. Commun.*, 2015, **51**, 6518–6520; (c) X. Gao, X. Li, L. Li, J. Zhou and H. Ma, *Chem. Commun.*, 2015, **51**, 9388–9390; (d) J. Liu, Y.-Q. Sun, Y. Huo, H. Zhang, L. Wang, P. Zhang, D. Song, Y. Shi and W. Guo, *J. Am. Chem. Soc.*, 2014, **136**, 574–577; (e) Y. Zhang, J.-H. Wang, W. Zheng,

ARTICLE

Journal Name

- T. Chen, Q.-X. Tong and D. Li, *J. Mater. Chem. B*, 2014, **2**, 4159–4166; (f) J.-T. Hou, J. Yang, K. Li, K. K. Yu, X.-Q. Yu, *Sens. Actuators B*, 2015, **21**, 492–100.
- 11 (a) S. Shahrokhian, *Anal. Chem.*, 2001, **73**, 5972–5978; (b) L.-Y. Niu, Y.-S. Guan, Y.-Z. Chen, L.-Z. Wu, C.-H. Tung and Q.-Z. Yang, *Chem. Commun.*, 2013, **49**, 1294–1296; (c) L.-Y. Niu, Y.-S. Guan, Y.-Z. Chen, L.-Z. Wu, C.-H. Tung and Q.-Z. Yang, *J. Am. Chem. Soc.*, 2012, **134**, 18928–18931; (d) H. Zhang, R. Liu, J. Liu, L. Li, P. Wang, S.Q. Yao, Z. Xu and H. Sun, *Chem. Sci.*, 2016, **7**, 256–260.
- 12 W. H. Melhuish, *J. Phys. Chem.*, 1961, **65**, 229–235.
- 13 M. J. Frisch, et al. Gaussian 09, Revision C.01; Gaussian Inc.: Wallingford, CT, 2010.



The fluorescence emission of benzothiazole derivatives (**1–3**) was efficiently tuned from green to red by elongation of π -conjugation. A white emission was successfully achieved from **3** in a polar-nonpolar binary solvent. By masking the phenol group in **3**, a novel NIR fluorescent probe for biothiols was constructed that allow to imaging application in living cells.